

# Bridging Seasonal Disconnectivity in Rural Rwanda: Economic and Environmental Impacts of Trailbridges\*

Cannon Cloud<sup>†</sup>

Goethe University Frankfurt

February 15, 2024

## Abstract

I measure the impact of trailbridges connecting rural Rwandan villages on remote-sensed developmental and ecological outcomes. Modern trailbridges provide safe and consistent commutes to work, school, markets and healthcare. To identify the causal effect of increasing villagers' mobility, I use variation in bridge construction timing and feasibility to compare villages in similar need of a bridge. The average treatment effect is a 3% increase in population, a 14% increase in night time light, and a 40% reduction in deforestation, indicative of improved biomass fuel market efficiency due to trade. Comparing villages on either side of the bridge by distance to all-weather roads reveals consistent effects. These findings underscore the value of completing missing pedestrian links with affordable infrastructure in fostering socio-economic development and environmental sustainability.

## 1 Introduction

Four out of five individuals with incomes below the international poverty line live in rural areas, giving the fight to eliminate global poverty a substantial spatial component (UNDESA, 2021). On one hand, space (e.g., large distances and difficult topography) is a developmental challenge to overcome—hampering rural labor and goods markets integration and leading to inadequate access to public services, infrastructure and social protection (UNDESA, 2021). On the other, space provides rural residents with their livelihoods in the form of agricultural activities, natural resources and ecosystem services (FAO, 2019).

In hilly and river-intersected rural regions with little infrastructure, high-quality trailbridges promise to overcome spatial isolation and eliminate uncertainty in access to and from otherwise remote villages. Evaluations of trailbridges in Nicaragua and Rwanda built by the non-profit Bridges to Prosperity (B2P henceforth) directly led to substantial wage earning increases (Brooks and Donovan, 2020; Thomas et al., 2021). Given the interdependency of the livelihoods of the extreme poor and the environment, and the potential unintended negative ecological effects of development programs (Heß et al., 2021) I look at spatial outcomes of trailbridges built from 2009 to 2022 in rural Rwanda, where in 2016 63% of individuals lived below the international poverty line of \$1.90 a day (The World Bank, 2020). Increasing connectedness through trailbridges led to a meaningful decrease in deforestation and an increase in night time light (henceforth

---

\*Cannon Cloud gratefully acknowledges Matthias Schündeln for advice and support, and Abbie Noriega and Bridges to Prosperity for their cooperation in providing data and context. Declarations of interest: none

<sup>†</sup>Cloud@econ.uni-frankfurt.de

NTL) radiance and remote-sensed, estimated population. The positive results of these relatively affordable infrastructure projects targeting missing links stands in stark juxtaposition to the road-heavy transportation budgets of developing countries and international donors. Despite the predominance of pedestrian and non-motorized transport in the developing world, only a fraction of budgets target pedestrian improvements (Kim and Dumitrescu, 2010).

In order to causally identify an effect, I use variation in bridge construction feasibility and timing to compare villages in similar need of a bridge. B2P identified more villages in need of a bridge than could be built immediately, while other villages have riverbeds with topographical features that precluded the construction of the types of bridges B2P built in the period from 2008-2022. Quasi-random rollout of trailbridges allows for estimation of effects in a difference-in-differences model. I provide evidence of parallel trends in pre-treatment outcomes using pre-trend estimates from Borusyak et al. (2021) that are robust to treatment effect heterogeneity and the Rambachan and Roth (2022) pre-testing problem. More so, deforestation results are consistent in magnitude when restricting the sample to sites with randomized construction dates from 2021 onwards taking part in a separate evaluation (Macharia et al., 2022). Including bridges built before randomization allows for measurement of medium term impacts, which is necessary to see effects on population and night time light. Results are also consistent when modifying parallel trend assumptions to allow linear or quadratic time trends or geographic cluster-year fixed effects.

The results are consistent with several likely mechanisms such as a substitution in land-intensive agricultural labor for wage-market labor, and better access to markets and mature wood-sources. The bridge facilitates more wage labor by decreasing costs/impediments from commutes. The resulting increased monetary income can decrease pressure on forests for resources (such as cooking fuel) and the substitution of labor reduces demand for farm land. Rwandans rely on biomass for fuel. When floods cut off villages, access to a large share of local woodlots is severed. Relying on forests on the same side of a bridge could result in more deforestation if there is not enough wood for the population or the forests are not ready for harvesting. Estimated population also increased, perhaps because villages are more attractive once better connected. Any new deforestation pressure from increased population is outweighed by other treatment effects. Population could by itself cause an increase in NTL, however there is still a significant increase in estimated NTL even while controlling for population. This suggests bridges increased NTL through other channels, such as increased incomes.

## 1.1 Background

## 1.2 Forest Use, Flooding and Bridges in Rwanda

Near sample trailbridges, canopy is predominantly agroforestry grown for biofuel, other forest products and ecosystem services. These trees are grown in rotation with or in and around crops (ERMA, 2021). In theory, cyclical deforestation is to be expected when trees are ready to be harvested, however, in practice, forest stocks (volume of wood) are extremely low from overuse and are often harvested too early (ERMA, 2021). More so, Rwanda is coming back from severe land degradation, and has pledged to rehabilitate 2 million hectares of land by 2030 (82% of land area) (ERMA, 2021). In the current context, a decrease in deforestation could be an indication of forests growing more efficiently. See section A Forest use in Rwanda for additional context relevant to deforestation outcomes.

Rwanda sees two rainy seasons between September to November and March to May, with a long dry season from June to August. Each rainy season, corresponds to the start of an agricultural season, though not all farmers squeeze in two seasons each year. Season A goes from September to February and Season B from March to June. The Western and Northern provinces have trended towards heavier precipitation events over the last 30 years, potentially

due to climate change. When coupled with recent deforestation and poor agricultural practices, heavy rainfall has led to the destruction of infrastructure such as buildings and bridges, as well as the loss of lives and crops (ERMA, 2021).

Beyond flood events, many Rwandan communities rely on inadequate bridges that are by design not functional throughout the year. Most common are timber bridges made of round logs laid next to each other with gaps in between, which are regularly overtopped or washed away during the rainy seasons. Even when in place many are unsafe to cross when waters are high (Shirley et al., 2021). Because over 83% percent of Rwandans live in rural areas and are reliant on walking for part of most trips (NISR, 2022), there is a major need for trailbridges to safely navigate Rwanda’s infamous hilly terrain. Shirley et al. (2021) identified over 1400 sites in Rwanda appropriate for the placement of an all weather bridge, of which only 3% had existing all-weather bridges. Given Rwanda’s size, this is approximately 1 bridge per every 17 square kilometers. Most of these crossings are over narrow streams where a small culvert bridge of 10 to 20 meters is sufficient, but over 20% of sites are in need of a substantial long cable bridge, such as the types B2P constructs.

When river flooding overwhelms current haphazard bridges, rural Rwandans are faced with substantial addition in travel times to schools, markets, healthcare services, and employment (Thomas et al., 2021), potentially fatal stream crossings, or a reduction in trips.

### 1.3 Background: Intervention

In order to provide reliable year round connections for remote villages, B2P in cooperation with the national and district governments has constructed 180 high-quality trailbridges in Rwanda from 2008 to 2023, primarily in the wetter and steeper western side of the country. After completion, each trail bridge becomes the property of the government of Rwanda with district governments providing maintenance. Until 2019, the identification of potential B2P trailbridge sites was ad hoc, but consistent in that the selection of trailbridges was determined through the reporting of sites without safe water crossings from residents and officials. From 2019, B2P chose sites from the 186 locations identified in the national needs assessments by Shirley et al. (2021), however construction timing remains ad-hoc for some of these. From 2021, 136 bridges are being built in a randomized order at the district level; see Macharia et al. (2022) for further discussion of the randomization process.

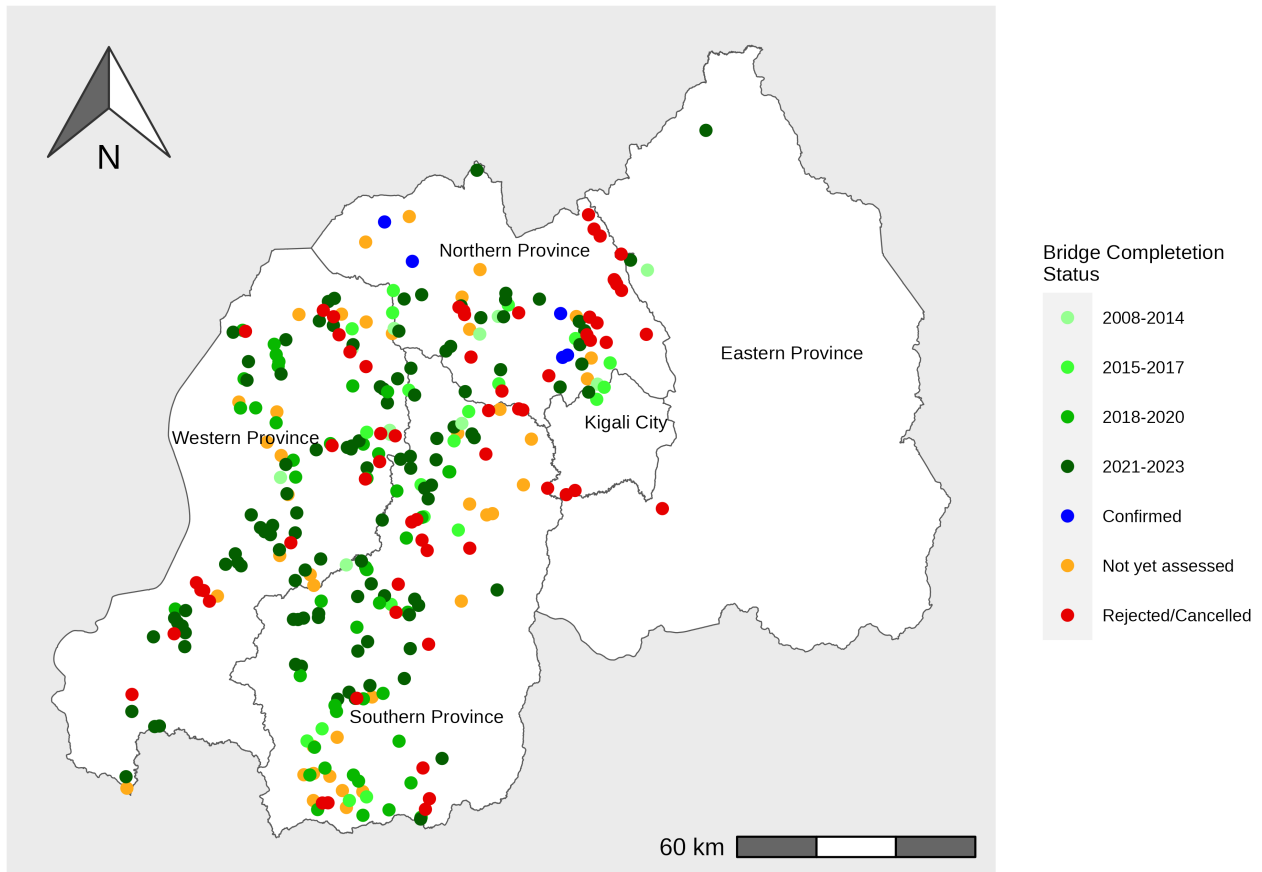
I look at bridges both before and after randomization to study treatment effects over a longer time horizon, and to validate effects found from the non-randomized construction with similar estimates from the randomized <sup>1</sup>. This study includes 267 sites that are either already completed, assessed by B2P to be in need of a suspension, suspended, or hybrid B2P type bridge, or included in the RCT. Figure 1 shows the location of all sites in Rwanda in the sample.

B2P had two standard designs for bridges to cut engineering costs and times. Suspended trailbridges hang from two foundations and require high (but accessible) sides for the necessary clearance. In flat areas, suspension bridges are needed. Their towers raise the cable on which the footpath is suspended, but the towers also need space for anchors on either end. A site might be technically rejected because one side is flat and the other elevated. In 2021, B2P incorporated into their standards a hybrid design, half suspended and half suspension, making it more feasible to connect a hill to a floodplain.

---

<sup>1</sup>I was aware of B2P randomizing some bridges in Rwanda starting in 2020, but was not aware of the details until Macharia et al. (2022) published their pre-analysis plan. Additionally, the two studies are looking at different outcomes with different units of observations over different time periods. I will incorporate additional randomized later-treated cohorts as data becomes available.

Figure 1: B2P's Water Crossing Sites in Rwanda by Status



Year label indicates time range trailbridge construction was completed. Rejected are sites deemed technically or socially infeasible for a trailbridge. Cancelled bridges were confirmed but then cancelled. Not yet assessed are sites that are identified from the national needs assessment, but a decision on bridge suitability has not yet been made through an assessment. Confirmed are agreed upon between the government and B2P but are not yet under construction. Graphic compiled by author. Bridge location and status data provided by B2P. Rwandan political boundaries provided by GLAD.

## 2 Data

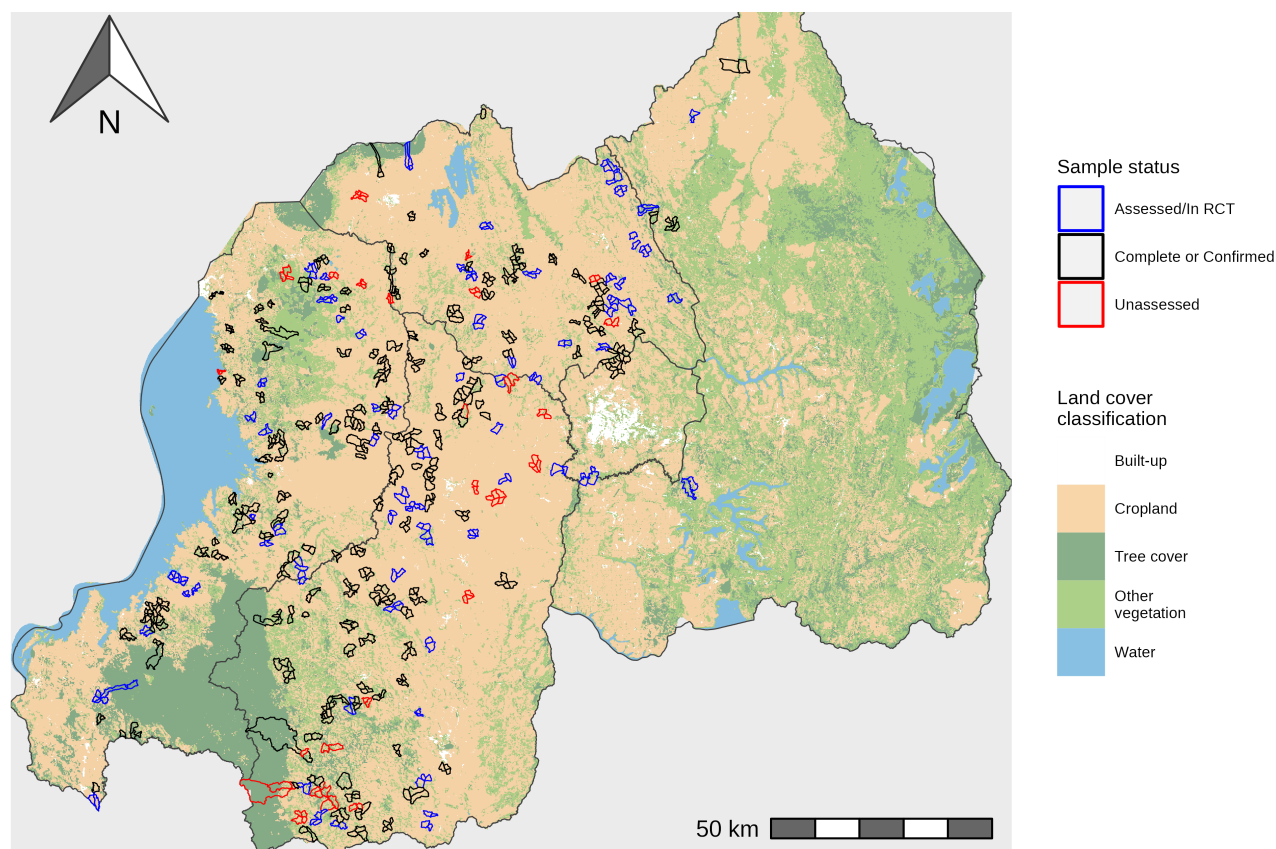
### 2.1 Bridge Data and Sample Selection

B2P tracks the status and location of each trailbridge site they have identified. If a site was eventually rejected, the reason for the rejection is recorded. Forty-three are rejected on technical grounds; the site is not appropriate for a standard B2P design. Eight were rejected for social reasons, for example the village preferred to wait for the construction of a vehicle bridge, or there was a failure to secure local funding. The specific rejection reason for three sites is not recorded. In addition, B2P tracks bridge type (which is determined by topographical constraints), as well as bridge span, estimated number of individuals served and completion date.

To focus on rural areas with significant canopy cover and an agricultural economy, as well as avoiding trends in night light and population movement driven by suburban expansion, I exclude sites that fall within the urban area of Kigali. Outside of the Kigali urban area, other bridge sites are predominantly rural and include only small built up areas. However, there are two peri-urban sites in Rubavu. According to FAO WaPOR land cover classification database, which reports the primary use of pixels at a  $100\text{m} \times 100\text{m}$  resolution, the median village adjacent to a trailbridge sites has zero built-up pixels, while the maximum has 11% (GFCD, 2015).

Figure 2 imposes the boundaries of villages adjacent to trailbridge sites over a mapping of land cover classification data in Rwanda, including built-up pixels. Black outlined villages

Figure 2: Land Cover and Bridge-Site Adjacent Villages



Shows boundaries of villages adjacent to B2P trailbridge sites. Black villages are completed or confirmed bridges. Blue villages are bridges assessed by B2P engineers to be in need of a B2P standard type bridge, or are included in the RCT. Red villages are identified sites that have not yet been assessed by BDP and are excluded from the sample for most specifications. Graphic compiled by author. FAO WaPOR Land Cover Classification data shows primary land use at 100m × 100m resolution. Rwandan political boundaries provided by GLAD.

have completed or confirmed trailbridges. The distribution of these treated villages falls along Rwanda’s steeper western half with high population densities and where montane forest was converted to intensively cultivated cropland. While not visible in Figure 2 as small forest plantations are grown in land primarily used for crops, the belt along which the bridges are built (the central plateau and Congo Nile Crest) is the center of Rwanda’s forest plantations (ERMA, 2021).

The blue outlined villages are not-yet or never-treated villages included in the sample for the main specifications. The red outlined villages are identified sites that have not yet been assessed by BDP and are not in the RCT. They are excluded from the sample from the preferred specification, in order to compare across sites with treatment dates as close as possible, but results are robust to their inclusion.

## 2.2 Village Boundaries

Data on political boundaries in Rwanda is provided by the Database of Global Administrative Areas (Hijmans, 2015). I use the fifth and smallest level of administration (the village level) as a unit of analysis for aggregating spatial statistics, such as yearly village-deforestation. The boundaries of villages often reflect topographical constraints such as streams, ravines, hills and mountains that physically restrict the movement of inhabitants. All completed trailbridges can be found at the perimeter of two or more villages, so village boundaries are the obstacles for the bridges to overcome. Using village boundaries as the unit of observation in an analysis concerning

spatial outcomes and spillovers is advantageous because the boundaries are meaningful in terms of geography, infrastructure and political and social networks with-in. Figure 2 illustrates the outlines of the villages included in the study sample.

## 2.3 Forest Data

Forest cover data is provided by the Global Forest Change Database 1.9 (GFCD henceforth), which reports percentage canopy cover for the year 2000 and deforestation from 2001 to 2021 (Hansen et al., 2013; GFCD, 2022). The data is reported at the pixel level, captured by Landsat satellites with 1 arc-second resolution. At the near equatorial latitudes of Rwanda, pixels are approximately  $30\text{m} \times 30\text{m}$ , or  $900\text{m}^2$ . Canopy is defined as vegetation over 5m in height and deforestation is reported as the year of deforestation event, i.e., a complete removal of all canopy in a pixel (Hansen et al., 2013).

For deforestation outcomes, I calculate the area of pixels that underwent a deforestation event weighted by the percentage canopy cover of the pixels in 2000, divided by the village area weighted by percentage canopy in 2000. For brevity, I refer to this as percentage deforestation of canopy, though it is not strictly correct as any deforestation of canopy in pixels where some canopy remains is not reported. Therefore, for any given year the estimate could under or over report relative to the actual amount of deforestation of the canopy. See figure X for a depiction of average deforestation over time by treatment status and how the normalization by canopy area affects the trends.

The areas surrounding future B2P sites are modestly forested, but primarily agricultural. FAO WaPOR land cover classification data reports the median village is 80% agricultural pixels. See figure 2 for an illustration of villages by FAO land cover classification. The median canopy cover of villages adjacent to bridge sites is 19% . The canopy is spread throughout the village area. The median village, 88% of pixels have at least 10% canopy cover. This dispersion is consistent with small woodlots and other agroforestry methods practiced by small farmholders in Rwanda (especially in the densely populated Central Plateau region (Mukuralinda et al., 2016)), as well as the occasionally larger institutional or public forest plantation. A handful of villages include sizable amounts of national parks with tropical montane rainforest. These areas differ in forest use, as the national parks are either protected entirely, or in the case of Nyungwe National Park has a buffer zone. This zone has since 2010 been under de jure management by the Rwanda National Forestry Authority for sustainable forest production and mitigation of impact of local communities (Gross-Camp et al., 2015).

Starting in 2013 GFCD improved their algorithms for deforestation detection. 2010 and 2011 data were revised with a worldwide 6% increase, but the jump in detection from 2013 onwards is much larger due to better sensors on satellites, creating non-linear discontinuities in the time series. The improvements were particularly better at detecting smaller scale changes, such as loss due to fires, selective logging and shifting agriculture (GFCD, 2022). This improvement is especially relevant in the case of Rwanda, where small woodlots and other agroforestry canopy is integrated sparsely throughout the study area.

See figure B.1 for illustration of deforestation between 2001 and 2021 in regions of B2P construction activity. Deforestation is most severe along the edges of the remaining heavily forested areas, but there is also deforestation distributed evenly throughout the study area which is predominately cropland. This is to be expected with the agroforestry practices of the land use systems in the Western and Northern parts of Rwanda (Mukuralinda et al., 2016).

## 2.4 Night Time Light Data

The NTL outcome analyzed is village radiant intensity in  $\text{mW}/\text{SR}$ . Annual NTL data from 2012-2022 is provided by the Earth Observation Group from the Visible and Infrared Imaging Suite

(VIIRS) (EOG, 2022). The annual time series is derived from a monthly aggregation of nightly data, and undergoes steps to correct for stray light, cloud masking, sunlit and moonlit pixels, and outliers driven by events like wildfires (Elvidge et al., 2021). The resolution of VIIRS NTL data is 15 arc seconds, or approximately  $500\text{m} \times 500\text{m}$  in Rwanda.

VIIRS resolution is 45 times smaller than the previous NTL data series, DMSP, and has superior low light imaging collection capabilities. These factors preclude including years earlier than 2012 with DMSP data. The sample villages are relatively small and dark. The median village in terms of area is slightly smaller than just 5 pixels of VIIRS data. For brightness, the Province of Kigali (which includes considerable rural areas) increased in radiance from 1.7 to  $4.1 \text{ nW/cm}^2/\text{sr}$  from 2012 to 2021. In contrast, the median radiance across all years of village clusters was  $0.17 \text{ nW/cm}^2/\text{sr}$ .

See Figure B.2 for an illustration of trends in NTL in the study area. Over the study period, the spatial spillover of ambient NTL from from brightening cities and towns is increasing. Ambient light from cities can be brighter than the median village in the sample. Because village treatment status and timing may not be independent of these spillovers, it is important to account for any differential trends due to location in estimation.

Stepping back from Rwanda, the relationship between rural economic activity and population density with NTL is a developing topic, especially for low-income countries. Gibson et al. (2021) advise “great caution” when using NTL data for studying low density rural areas, finding that even VIIRS was not a suitable measurement for GDP outside of cities in the context of Indonesia. However, Pérez-Sindín, Chen, and Prishchepov (Pérez-Sindín et al.) found VIIRS NTL data capable of detecting long-term patterns of socioeconomic change for municipalities in Colombia, the second level of administrative units. They found that VIIRS data predicted regional domestic product (RDP) with an  $R^2$  of .309 for rural municipalities with populations under 5,000, compared to .873 in cities over 500,000. They even found NTL predicted RDP in areas with population density as low as 31 persons per  $\text{km}^2$ , but found poor performance in regions with heavy canopy obscuring lights. Rwanda, in contrast, is not heavily forested (as discussed earlier) and has a high population density even in rural regions, but Rwandan villages, at the fifth administrative unit, are much smaller than Colombian municipalities.

## 2.5 Population Data

The population outcome of interest is the log of estimated population. WorldPop (2022) provides an annual gridded population distribution dataset at a  $100\text{m} \times 100\text{m}$  resolution from 2000-2020, based on the methods from Lloyd et al. (2019). Census data from 2012, in this case at the third “sector” level (two levels above village), is disaggregated with a flexible random forest estimation technique (Stevens et al., 2015). Multiple geospatial datasets on topography, infrastructure, buildings, waterways, climate, NTL, and land-cover classification create a prediction layer which is used as weights for the dasymetric redistribution of aggregated census counts.

The accuracy of the estimation is dependent on the age, accuracy and aggregation of the input data. For Rwanda the census data is from 2012 and the disaggregation is only at the sector level. One time varying input of the WorldPop data is VIIRS NTL data, which this study independently examines.

Figure B.3 shows change in population by hectare for the area of Rwanda including the sample sites. Spatial spillovers from cities appear smaller than from NTL. Highways do not stand out like they do in the NTL data, and their are pockets of large rural population increase such as north of Nyanza and around Byumba that are less prominent in NTL data. The  $R^2$  of regressing estimated population on NTL is 0.17, so clearly estimated population is not simply NTL data repackaged one for one.

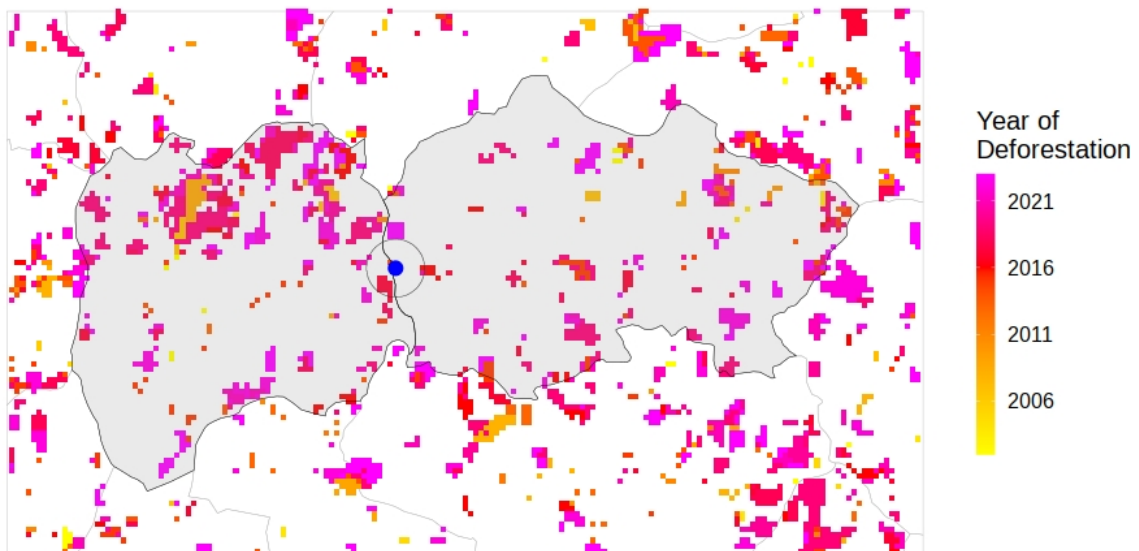
### 3 Empirical strategy

#### 3.1 Spatial Specifications for Analysis

In order to measure the treatment effect of a trailbridge it is necessary to choose the area over which to aggregate spatial statistics. Because bridges are built at the site of topographical constraints and not at the center of treated communities, too narrow a bandwidth and there is a risk the treated community falls outside. Too wide a bandwidth could include areas that are only marginally effected by a trailbridge or not at all if the area is on the other side of a boundary like a rivers or a hill. Including much untreated area would make it harder to detect a treatment effect as the effect will be mechanically smaller (averaged over a larger area) and there will also be more statistical noise.

The main specification aggregates spatial data at the village level. Analysis of adjacent villages takes into account meaningful geographic constraints and the social and spatial ties that led to that area being designated an administrative entity. I first looks at the average effect for all villages on either sides of the bridge, regardless of intent to treat. Then, I perform heterogeneity analysis, comparing by each bridge villages furthest and closest to all-weather roads. However, village observations vary in area and distance from the bridge site. Analysis of buffer zones ensure observations are consistent in area, but are insensitive to boundaries or differences in settlement patterns. More so, by definition buffers span both sides of the bridge. The choice of a buffer with a 1km radius was chosen in rough equivalence to the median area of a bridge-adjacent village at  $1.19\text{km}^2$ . Since the median bridge site is placed adjacent to three villages, the 1km radius captures a large portion of adjacent villages in all directions.

Figure 3: Spatial Specifications for Analysis



Black outlines illustrate villages over which spatial statistics are aggregated. Light gray lines show surrounding village boundaries not included in the sample. The bridge site is demarcated by a blue dot. A radius of 150m from the bridge is displayed with a dark gray circle. Deforestation provided for illustration; data from GFCD. Rwandan political boundaries provided by GLAD.

Figure 3 illustrates an example bridge site and how the units of observations are determined for the village specification. The black outlined shapes show the boundaries villages, while the light gray fill shows what areas are included in aggregating spatial statistics. Yearly deforestation

is displayed as an example. Villages adjacent to the bridge site (with borders within 150m) are included in the analysis. Spatial statistics are aggregated for each village. If a village is adjacent to two sites, treatment is defined by the year of completion of the first bridge. In some years, a never-treated or not-yet-treated site-adjacent village borders a treated village, which may allow some spatial spillovers, depending on the topography.

### 3.2 Identification Strategy

To analyze treatment effects, I use variation in treatment timing, also known as a staggered rollout. Standard two-way fixed-effects estimators can be biased with staggered treatment timing and heterogeneous effects (Goodman-Bacon, 2021). Given the wide range of factors that could dynamically affect treatment intensity across trailbridge sites such as remaining forest canopy, population growth and village area, it is credible those conditions apply. Therefore, I use a robust event-study estimator by Borusyak et al. (2021) that still accounts for unit (village or buffer) and period (year) fixed effects, and can incorporate unit linear or polynomial time trends. These effects control for confounders that are either relatively stable across time (e.g., village culture and leadership, canopy cover, distance to market) or space (e.g., weather, technology, population growth, national policies). Allowing unit or district specific trends can control for differential trends across trailbridges (e.g., varied population growth, suburban expansion), but requires specifying a correct functional form.

Borusyak et al. (2021) show estimates are unbiased if parallel trends hold across units and there is no anticipation of treatment effects. Anticipation effects in this context would seem unlikely or marginal as trail-bridges are non-fungible, and because bridges provide a physical service it is hard to benefit from it before it is built. However, B2P does employ local labor in the construction of the bridge, which could substitute for agricultural labor for some. In addition, individuals might accept temporary longer commutes to work in the case of a flood if they know a bridge will come soon, affecting labor market decisions. Because these potential anticipation effects work through the same mechanisms as theoretical bridge effects, they would bias effects towards 0.

The assumption of parallel trends is the most crucial in the context of this sample. Only half of the sample is being built in a randomized order, and only from 2021 onwards. Our identification strategy assumes that village-specific treatment timing is exogenous to outcomes conditional on village and period fixed effects. This is plausible as bridge construction timing was largely determined by factors such as terrain difficulty, proximity to other B2P sites, and eager district government officials. If B2P non-random selection was correlated with changing trends in outcomes (e.g., faster developing areas were prioritized) this would bias results, but this does not seem to be the case. In more technical terms, sufficient conditions for the assumption to hold are that the selection mechanism is independent from village-time-varying unobservables and that village-time-varying unobservables that affect outcomes have a constant mean over time conditional on village-level time-invariant unobservables (Ghanem et al., 2022). Most bridges built after 2021 were built in a randomized order within district, but have less years of outcome data.

The data are annual time series, so treatment start is defined as the rounded year of bridge completion, i.e. a bridge completed before September is considered treated that year, and September onwards is considered treated next year. More than half of bridges constructed in the latter half the calendar year were completed in November and December, and Rwanda's planting season begins in September with harvests in January and June. Because the rural Rwandan economy is primarily agricultural, I expect outcomes from trailbridges to be noticeable during or after harvest. Additionally, deforestation occurring late in the year is often attributed to the next year, especially in cloudy regions with few quality satellite photos like Rwanda once the rainy season starts in December (Potapov and Weisse, 2022).

I assume outcomes in each village or buffer period are described by

$$\text{outcome}_{it} = \alpha_i + \beta_t + \gamma_{it} + \tau_{it}d_{it} + \varepsilon_{it}, \quad (1)$$

where  $\text{outcome}_{it}$  is either percentage deforestation, log total population or total NTL radiance,  $\alpha_i$  is a village fixed effect,  $\beta_t$  is a year fixed effect, and  $\gamma_{it}$  is a (sometimes included) village or district time trend that can be linear or polynomial. Treatment is designated by  $d_{it}$ , a village-year indicator, and  $\tau_{it}$  is the village-year-specific treatment effect. The error term,  $\varepsilon_{it}$ , captures yearly-village random variation in the observed outcomes that is unrelated to treatment, e.g., measurement error due to clouds or wildfires started by lightning.

Conditional expectations of treatment effects  $\tau_{it}$  can be estimated for different estimands of interests. These estimands could vary over time, (e.g., the average treatment effect across all post-treatment months  $\mathbb{E}[\tau_{it}]$  or the average treatment effect within 2 years of trail bridge completion year  $c_i$ ,  $\mathbb{E}[\tau_{it}|t \leq c_i + 1]$ ) or over space (e.g., the average treatment effect weighted by village area).

I take the natural logarithm of population, which has several benefits. Effect sizes are likely relative to disparate baseline levels, and the estimates can be interpreted as semi-elasticities, i.e., the percentage increase in population due to trailbridge construction. Deforestation outcomes, which are predominately 0, are normalized by dividing by village, forested pixels or canopy area, and can be interpreted as yearly percentage increases in levels or summed for aggregate effects. NTL radiance is calculated from the sum of radiance aggregated across the observational area.

Standard errors are clustered at the adjacent trailbridge site level, which can include multiple trailbridges if they have bordering villages. For estimation of residuals, I assume constant treatment effects within cohorts, defined by construction completion date into six similar sized group. Standard-errors are computed using a leave-out procedure. In principal, imposing constant treatment effects over larger groups leads to more conservative inference (Borusyak et al., 2021).

## 4 Results

### 4.1 Night Time Light

Table 1, column 1 reports the average treatment effect across all treated village-years. The sum of village NTL radiance increased on average by  $0.51 \pm 0.26\%$  (mean estimate  $\pm$  std. error). The effect is rather large compared to mean pre-treatment, but over the study period the sample grew much brighter. Column 2 is the preferred specification, which incorporates linear-unit time trends. The estimate is more precisely estimated as  $0.47 \pm 0.18\%$ . Treated villages before 2013 are dropped in order to estimate trends. Unlike cluster-time trends that use data points (untreated observations) in their calculation, unit trends are extrapolated from just the untreated periods of the unit. In this case, the maximum number of post-treated periods is 6, so the assumption of continuous linear trends is not extended very far.

Column 3 only includes villages outside of the RCT so not built in a randomized order. The estimate,  $0.54 \pm 0.17\%$ , is similar to the estimate for the entire sample. On the other hand, Column 4, which only includes villages in the RCT, finds no effect  $0.00 \pm 0.14\%$ . This makes sense, as theory would suggest treatment effects would grow with time as incomes are converted to goods that emit lights. There are currently only two years of randomization data for night time light data, and I will update the results with new data for 2023 when available.

Figure 4 provides evidence that there is a gradual onset of the treatment effect for night time light. Effects for villages for both randomized and non-randomized bridges are similar for the first two years. However, as the results are both close to zero, this does not inspire much confidence in the integrity of the larger estimates for period 3 onwards of the non-randomized

Table 1: Estimated Treatment Effects for Radiant Intensity in mW/SR

	(1)	(2)	(3)	(4)
	NTL sum	NTL sum linear village time trends	NTL sum. linear village time trends non-randomized	NTL sum, linear village time trends randomized
Treatment-estimate	0.51** (0.26)	0.47*** (0.18)	0.54*** (0.17)	-0.00 (0.14)
Pretrend-1	-0.08 (0.15)	-0.09 (0.10)	-0.09 (0.10)	0.09 (0.15)
Mean pre-treatment	3.02	3.02	3.02	4.58
Treated obs.	1095	1095	952	143
Total obs.	7282	7282	7139	2016
Treated villages	297	297	190	107
Total villages	662	662	662	336
Treated bridges	113	113	73	40
Total bridges	266	266	266	136
Year from	2012	2012	2012	2017
Year to	2022	2022	2022	2022

*Notes:* \*  $p < 0.1$ , \*\*  $p < 0.05$ , \*\*\*  $p < 0.01$ . Col. 1–4 include controls sites either rejected after further assessment by B2P engineers, currently confirmed for construction, or in the RCT. Col. 1–4 estimate effects on village area sum of night time light radiant intensity in mW/SR. Standard errors are in parentheses. The standard errors are computed using the leave-out procedure recommended in Borusyak et al. (2021). Cohorts are constructed by combining treatment years from 2008 onwards so that each cohort has at least 15 bridges. All estimates account for year fixed effects and village fixed effects. Col. 2–4 additionally account for unit-linear time trends. One large outlier (a national park forest lit by highway lights), is dropped from all columns.

data. Instead, the pre-trend coefficients provide evidence of parallel trends holding between controls and treated, at least for before the onset of treatment.

In this instance the OLS/TWFE results are similar to the Borusyak et al. estimates with linear time trends, but have smaller standard errors.

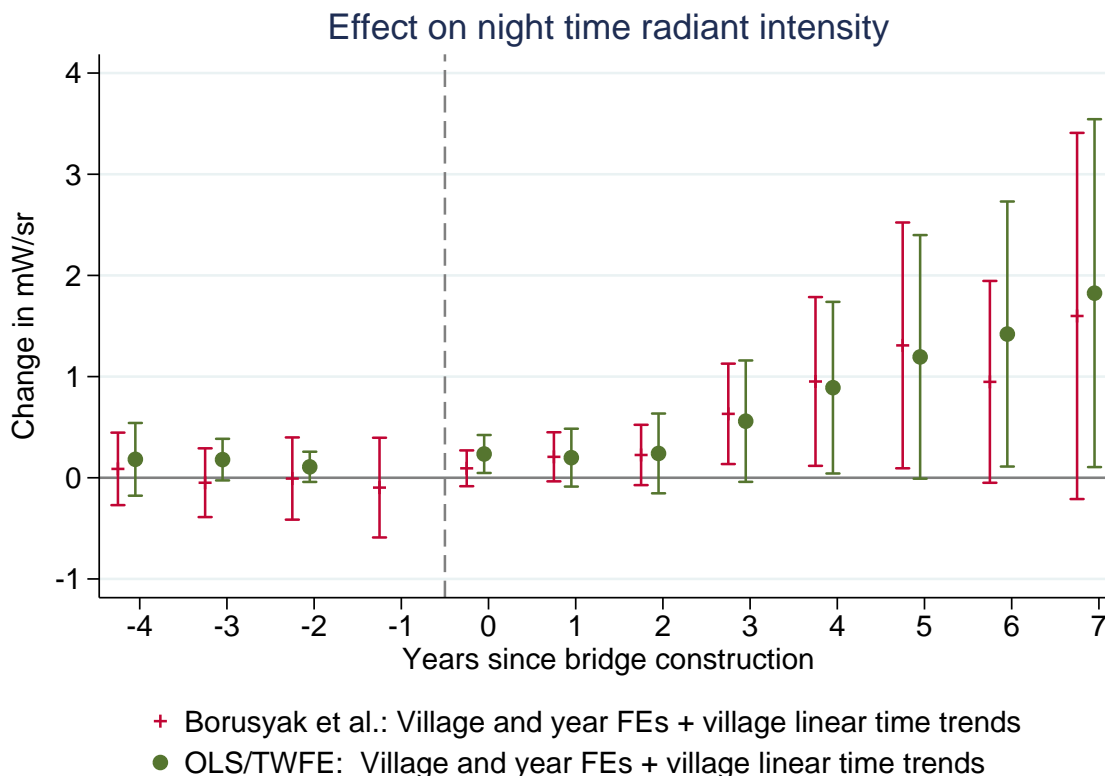
The results are robust to taking the log of NTL radiant intensity plus 0.1, which transforms the data so the yearly mean increases linearly instead of exponentially. The resulting coefficient equates approximately to a 20-25% increase for a median village post treatment. The results are similarly robust to taking the square root of village radiant intensity, or dividing by village estimated population.

## 4.2 Estimated Population

Table 2 reports estimated treatment effect on remotely-sensed village population. Column 1 reports estimates using (perhaps naively) just village and year fixed effects, and estimates an increase of approximately 2% averaging across all treated village-year observations. In column 1 the panel begins in 2012 in order to minimize the number of years the assumption of parallel trends most hold, but three villages adjacent to one bridge built in 2008 must be dropped. As populations are relatively stable, estimated village fixed effects using just one period are relatively more accurate than for noisier outcomes like deforestation.

Column 2 is the preferred specification, incorporating linear village time trends, which can, if modeled correctly, correct for confounding trends. The panel is extended backwards in order to accurately calculate parallel trends. Starting the panel too early risks missing more recent changes in trends, while starting the panel too late risks over-fitting on fluctuations between years. The estimated population variable appears to have considerable noise, relative to the

Figure 4: Yearly Treatment Effects on Night Time Light Radiant Intensity and Pretrends



+village linear time trends indicates inclusion of linear-village time trends. The 95% confidence intervals are indicated by bars. Standard errors are clustered at the bridge site-cluster level and are computed using the recommended leave-out procedure recommended. Cohorts are grouped by their trailbridge construction date. Estimates account for year fixed effects and village fixed effects.

effect size. I choose 2007, but the results are robust to starting the panel between 2000 and 2011. The estimated population increase across all treated observations is  $0.034 \pm 0.013\%$ . Because the population data currently ends in 2020, I can not estimate the effect on the part of the sample in the RCT, since those are constructed from 2021 onwards.

Figure 5 shows yearly treatment effects and pretrends on log population. Like night time light, the effect grows with time. Pre-trends provide evidence of parallel trends between treated and control villages holding for another variable (population growth), at least for the period before treatment onset.

### 4.3 Deforestation Outcomes

Table 1, column 1 reports the average treatment effect across all treated village-years. The area of deforestation as a percent of village canopy decreased on average by  $-0.17\% \pm 0.07\%$ . To put the trailbridge programs aggregate estimated effect into perspective, the median village has 30 hectares of canopy, so the effect size implies a decrease in canopy loss of  $510\text{m}^2$  yearly. Relative to the pre-treatment mean of yearly deforestation, this is an approximate 46% decrease.

Because of discontinuities in the GFCD time series, and to minimize the number of years the assumption parallel trends needs to hold over, columns 1 and 2 begin the panel in 2011.

Column 1 includes all treated observations, and uses year and bridge-cluster site fixed effects. The specification uses interacted year and district<sup>2</sup> fixed effects to capture variation in common

<sup>2</sup>In five instances there were no controls remaining in a district, so those districts were combined with the nearest neighboring district based off the location of the bridges. The district with the most sites that was combined had only 5 bridges.

Table 2: Estimated Treatment Effects for Estimated Population, Village Specification

	(1)	(2)
	Log population	Log population linear time trends
All-treated-years	0.021 (0.015)	0.034** (0.013)
Pretrend-1	0.003 (0.007)	0.001 (0.004)
Mean pre-treatment	6.55	6.50
Treated obs.	630	654
Total obs.	6066	9464
Treated villages	187	189
Total villages	674	676
Treated bridges	71	72
Total bridges	270	271
Year from	2012	2007
Year to	2020	2020

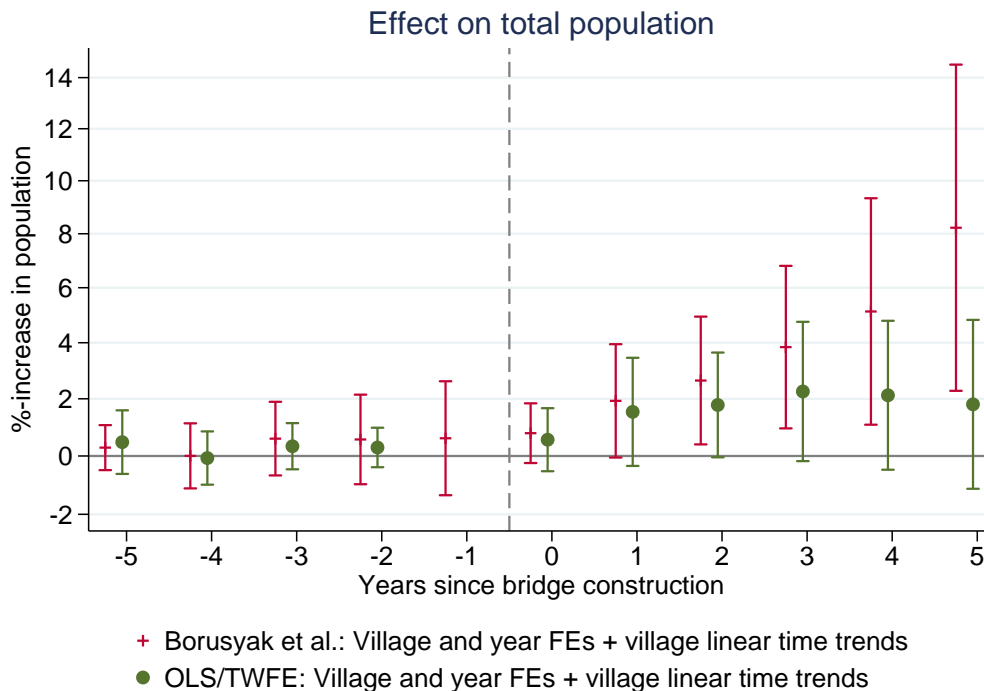
*Notes:* \*  $p < 0.1$ , \*\*  $p < 0.05$ , \*\*\*  $p < 0.01$ . Col. 1-2 and 4 display numbers that are untransformed coefficient estimates from a log-linear specification. All columns rely on as controls sites that were rejected only after further assessment by B2P engineers. Col. 1-2 and 4 estimate effects on the log of village estimated population, col. 3 on the village population, and col. 5 on yearly changes in population. Standard errors are in parentheses. The event-study's standard errors allow for clustering of the model error at the site cluster level and are computed using the leave-out procedure recommended in Borusyak et al. (2021). Cohorts are grouped by their two years trailbridge construction window, except 2015 and before are grouped as one. All estimates account for year fixed effects and village fixed effects. Time trends are calculated at the village level.

Table 3: Estimated Treatment Effects for Percent Canopy Deforested

	(1)	(2)	(3)	(4)
	%-canopy deforested Main sample year#district FEs	%-canopy deforested Non-randomized year#district FEs	%-canopy deforested Randomized year#bundled- district FEs	%-canopy deforested Randomized year and district FEs
Treatment-estimate	-0.17*** (0.07)	-0.19*** (0.07)	-0.31** (0.16)	-0.18 (0.13)
Pretrend-1	0.01 (0.06)	0.01 (0.06)	-0.01 (0.12)	0.16 (0.13)
Mean pre-treatment	0.37	0.37	0.40	0.40
Treated obs.	1181	1038	143	143
Total obs.	8088	7945	1348	1348
Treated villages	306	199	107	107
Total villages	674	674	337	337
Treated bridges	116	76	40	40
Total bridges	270	270	136	136
Year from	2011	2011	2019	2019
Year to	2022	2022	2022	2022

*Notes:* \*  $p < 0.1$ , \*\*  $p < 0.05$ , \*\*\*  $p < 0.01$ . Col. 1-2 include controls sites either rejected after further assessment by B2P engineers, currently confirmed for construction, or in the RCT. Col. 3-4 only use sites in the RCT as controls. Col. 1-4 estimate effects on yearly percent canopy cover deforested, calculated as the yearly village area deforested weighted by percent canopy cover of the deforested pixels in 2000 and divided by total village area forested in 2000. Standard errors are in parentheses. The standard errors are computed using the leave-out procedure recommended in Borusyak et al. (2021). Cohorts are constructed by trailbridge construction date so that each cohort has at least 15 bridges. Col. 1-3 account for year fixed effects, bridge cluster fixed effects, and interacted year and district fixed effects. Col. 4 controls for year and district fixed effects.

Figure 5: Yearly Treatment Effects on Log Population and Pretrends, Comparing Time Trends



Linear time trends are estimated at the village level. Estimates derived from a panel spanning 2007-2022. The 95% confidence intervals are indicated by bars. Standard errors are clustered at the bridge site-cluster level and are computed using the recommended leave-out procedure recommended. Cohorts are grouped by their trailbridge construction date. Estimates account for year fixed effects and village fixed effects.

in time for spatially proximate sites not shared across the country, such as wildfires, drought, or expanding local towns. If any of those spatial confounders were correlated with treatment assignment, uncontrolled results could be biased. Column 2 narrows the set down to treated observations that were not part of the RCT and reports a similar estimate, which is not a surprise as the samples are not much different. Column 3 only includes treated observations taking part in the RCT and estimates a larger impact  $-0.31\% \pm 0.16\%$ . Column 3 also includes interacted year and district fixed effects, but because of the smaller set of controls I bundle the original 20 districts into 5 based on the proximity of the bridges. Column 4 shows a parsimonious specification, dropping bridge-cluster fixed effects entirely and replacing them with a much larger unit of aggregation, the district. In theory this is the minimum identifying specification, based on the knowledge that the bridges were randomized within district. However, the large pre-trend estimate reveals that there may be something amiss. While randomization was randomized within district, rollout of construction by district is not random, as B2P needs the cooperation of sometimes otherwise engaged district officials. A difference in deforestation trends across districts would bias results. Column 3, which can flexibly account for spatial trends by bundles of neighboring districts, appears to outperform column 4 when using pretrends as a metric.

District-year fixed effects capture more granular covariation in time, without making assumptions about covariation across periods, such as village- or district-time trends. I avoid unit-time trends all together because they overfit the deforestation data, either predicting highly negative or positive trends or none at all. Secondly, projecting linear trends across the non-linear change in outcomes in 2011 and, especially, 2013, seems, a priori, a bad fit of the data generating process even if time-fixed effects soak up part of the shift. However, in practice, including either linear or quadratic cluster-time trends produces a similar result to Column 2 (not shown), with estimated cluster-time trends not so different from each other.

Spatially enlarging the pool of observations for calculating unit fixed effects could increase accuracy, but at the cost of assuming that deforestation patterns of a village are alike between spatially proximate villages. Replacing trailbridge-cluster site fixed effects with smaller and larger units of aggregation like village, or district makes only marginal difference in estimates (not shown). Removing unit fixed effects entirely only modestly decreases the coefficient and significance (result not shown). Having only year fixed effects tightens the parallel assumption to identical-in-levels, which given the similarity in outcomes before treatment (see Figure X), is not entirely implausible.

Unit fixed effects for treated villages are derived from only pre-treatment observations. Because there is a large jump in deforestation in 2013, village fixed effects for treated observations are biased downwards commiserate with the number of pre-treatment periods from before 2013 included. Theoretically, this should not bias the treatment effect with parallel trends because the systematic over and under estimation balances out, but it could increase standard errors. The similarity of column 2 and 8 indicate unit fixed effects barely effect outcomes, so underestimated village fixed effects for the treated are likely not a concern.

This paper has presented a number of different estimation models relaxing parallel trends (e.g., cluster time trends, cluster-year fixed effects) and strengthening assumptions such removing village fixed effects (balanced in outcome levels), and found consistent estimates on percent canopy deforested yearly; around 0.17 for the entire sample and pre-RCT sites and slightly higher, 0.3, for the RCT sites. The continuity between these models suggests that the parallel trends condition holds, and even the far more stringent balanced-in-levels assumption is plausible.

Estimating pre-trend coefficients can also provide evidence of parallel trends. Figure X is an event plot showing estimated treatment effects for each year both after and before treatment. Standard OLS/TWFE estimates and the robust difference-in-differences BSJ estimator. The estimators show qualitatively similar results, but yearly treatment effects are larger for the BSJ estimator. This can be partially explained by normalizing the estimates to period -1 for the OLS/TWFE models, which could bias estimates due to anticipation effects or random noise in that period. The difference between OLS results and the BSJ estimator, and the generally increasing estimates with time, suggest that there are dynamic treatment effects.

The pre-trend coefficients provide additional evidence of parallel trends for another variable.

## 5 Heterogeneity Analysis

Until now, all specifications estimated treatment effects with villages or pixels from both sides of the bridge, aggregating the effects of being on the close side or the far side of the bridge together. In some cases, bridges are clearly of equal importance in both directions, e.g., connecting a health clinic on one side to a school and market on the other. In other cases, one side is clearly disconnected, while the other is well integrated into a major road system.

Table 4 shows treatment effects for villages by bridge site which are furthest and closest to an all-weather road. The distance is measured from a point 100m away from the bridge location towards the centroid of the village polygon. What is fascinating, is that the bridges were built with the intention of treating more remote villages, but the effect on villages on the near side of the bridge are equivalent to the remote villages.

## 6 Discussion

Treatment effects should be considered intent-to-treat. While compliance with a bridge is hard to avoid, there are three trailbridges that went out of service, only one of which was replaced by B2P. Additionally, trailbridges might be placed in a location that is not convenient for all

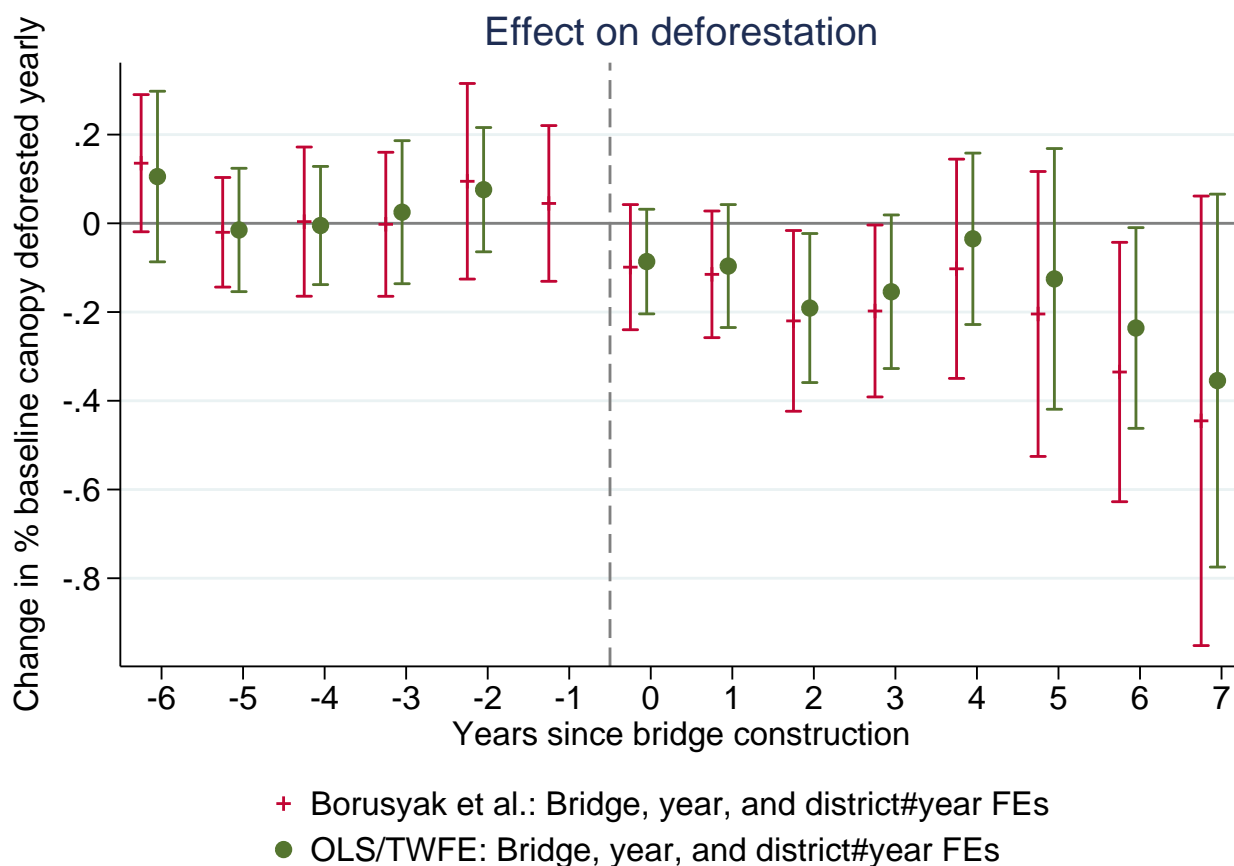
Table 4: Heterogeneity by Distance to an All-Weather Road

	(1) Night time radiant intensity	(2) Log of total population	(3) % canopy cover deforested
Far-Village	0.61*** (0.17)	0.03*** (0.01)	-0.18*** (0.07)
Close-Village	0.55*** (0.20)	0.04*** (0.01)	-0.18*** (0.07)
Difference	0.06 (0.19)	-0.01 (0.01)	0.00 (0.06)
Pretrend-1	-0.09 (0.10)	0.00 (0.00)	0.00 (0.06)
Mean pre-treatment	3.03	6.50	0.37
Treated obs.	802	497	868
Total obs.	6879	9148	7655
Treated villages	218	142	225
Total villages	652	666	664
Treated bridges	112	72	115
Total bridges	262	267	266
Year from	2012	2007	2011
Year to	2022	2020	2022

*Notes:*

*Notes:* \*  $p < 0.1$ , \*\*  $p < 0.05$ , \*\*\*  $p < 0.01$ . Col. 1–3 include controls sites either rejected after further assessment by B2P engineers, currently confirmed for construction, or in the RCT. Standard errors are in parentheses. The standard errors are computed using the leave-out procedure recommended in Borusyak et al. (2021). Cohorts are constructed by combining treatment years from 2008 onwards so that each cohort has at least 15 bridges. Col. 1–2 account for year and village fixed effects, as well as village linear time trends. Col. 3 accounts for bridge cluster, year, and interacted district-year fixed effects.

Figure 6: Yearly Treatment effects and Pretrends, Full Sample from 2011-2022



Includes the main sample from 2011-2022. The 95% confidence intervals are indicated by bars. Standard errors are clustered at the bridge site-cluster level and are computed using the recommended leave-out procedure. Cohorts are grouped by their trailbridge construction date. Estimates account for year fixed effects and bridge-cluster site fixed effects.

village residents.

The findings should be interpreted as short to medium run effects, but not long. The number of trailbridges with more than seven years of data is only thirteen. Additionally, the preferred estimates of treatment effects on both population and night time light data relied on the assumption of extended counterfactual trends, which grow less credible further away from treatment start.

The decrease in deforestation and increase in night light (even when controlling for population) are in line with a theory of shifting labor practices, from agricultural to wage work. Decreased demand for agricultural land would allow woodlots to grow for longer and more efficiently before being turned over for agricultural production. However, there are competing theoretical mechanisms for the reduction. Perhaps villages are no longer forced to prematurely harvest understocked woodlots for cooking fuel when floods had previously cut them off from a substantial share of nearby wood sources. This would explain the decrease in deforestation on both sides of the bridge. Expected decreases resulting from shifts in labor would be much larger on just one side. Population increases reflect the increased desirability of living close to the bridge as it dramatically increases the number of locations that can be easily reached by foot. Increased night light could be caused by increased incomes of former residents, and also by settlement of new residents and businesses now that the location is more desirable.

The estimated treatment effect for percent of canopy deforested is substantially driven by modest to large sized yearly village deforestation occurrences. Appendix Table X shows no

treatment effect on the likelihood of there being a deforestation event, so the decrease in deforestation is being driven by less large deforestation events when they do occur. Additional heterogeneity analysis by percent canopy cover, preferably with newer data than 2000, is needed to get a clearer picture of what type of forest land is being less deforested. Additional analysis of forest growth could collaborate if deforestation reduction is driven by letting woodlots mature more efficiently.

Extrapolating from survey findings in Nicaragua and Rwanda (Brooks and Donovan, 2020; Thomas et al., 2021) that found bridges increased wage income and movement out of agriculture, this paper contributes to the literature on the context specific income effects on deforestation in rural developing countries. For example, unconditional cash transfers in Sierra Leone (increasing income without employment) led to a crowding-in of the agricultural sector and an increase of clearance of young growth (Wilebore et al., 2019). In Mexico, conditional cash transfers based on child health and educational decisions led to increased deforestation in isolated areas. Raised incomes increased demand for land-intensive goods, and where there was not market access, households extended their ecological land-use footprint (Alix-Garcia et al., 2013). Lastly, in Pakistan cash transfers shifted fuels sources away from forest products and towards modern fuels (Nawaz and Iqbal, 2020). Taking these studies into context, perhaps the new year-round connectedness to mature fuel sources and a shift in labor from agriculture result in less deforestation even when incomes and, assumedly, demand for land-intensive goods goes up.

At face value, the reduced deforestation results lead to the preservation of valuable ecosystem services—a gross ecological benefit. For example, forests are a valuable asset in preventing erosion in the hilly and increasingly, due to climate change, flooded Rwanda countryside. More than 70% of all land in four of the districts where B2P constructed bridges are at very high and extreme risk of soil erosion (ERMA, 2021). However, general equilibrium effects can not be ruled out. In net, if raised income increases demand for land-intensive goods, then the ecological consequences could be shifted elsewhere. However, if the reduction in deforestation is caused by more efficient forestry practices, then it is clearly a gain. Additionally, purchases of fuel or other goods at now more-accessible markets would provide a net benefit if those goods are produced more efficiently.

It has been well documented that rural roads and trunk roads lead to a shift towards nonfarm employment, but a study focusing on rural roads in India found no effect on population, incomes or assets (Asher and Novosad, 2020). Perhaps this can be explained by the fact that bridges have a more profound impact on transportation times for foot traffic than roads. Roads without additional transportation are at best a marginal improvement.

The positive results from the paper also put into question the funding priorities of many developing country governments and international donors. Despite the predominance of foot travel in the rural developing world and the relative affordability of non-motorized transport infrastructure, only a fraction of investment goes to ensuring safe and efficient pedestrian routes (Kim and Dumitrescu, 2010; Jennings, 2016).

Lastly, this paper contributes to the literature of using NTL data to detect development. Making use of recent high-resolution and higher quality NTL data allows for novel comparisons of relatively small and dark units of observations (rural villages in Rwanda) with only a modest underlying change in income and population.

## 7 Extensions

In the future, this paper aims to incorporate, among other analysis, heterogeneity results of treatment intention from B2P.

The increase in night time light is not calibrated to any income or wealth scale. Making that connection would allow for a estimation of the monetary benefit of the project. Time-series of

estimated wealth using remote sensing data at the scale needed are currently prohibitively expensive. There are other high resolution wealth datasets available for one period. The drawback would be to assume that relations about wealth and night time light that hold across space also hold across time.

Additionally, the deforestation analysis is currently one-sided. Incorporating data on afforestation or changes in tree density would provide collaborative evidence of a shift from agriculture or more efficient management of forest plantations. Lastly, incorporating detailed data on land use and could provide insight into the mechanisms driving changes in deforestation.

## References

- Alix-Garcia, J., C. McIntosh, K. R. Sims, and J. R. Welch (2013). The ecological footprint of poverty alleviation: evidence from Mexico’s Oportunidades program. *Review of Economics and Statistics* 95(2), 417–435.
- Asher, S. and P. Novosad (2020). Rural roads and local economic development. *American economic review* 110(3), 797–823.
- Borusyak, K., X. Jaravel, and J. Spiess (2021). Revisiting event study designs: Robust and efficient estimation. *arXiv preprint arXiv:2108.12419*.
- Brooks, W. and K. Donovan (2020). Eliminating uncertainty in market access: The impact of new bridges in rural Nicaragua. *Econometrica* 88(5), 1965–1997.
- Elvidge, C. D., M. Zhizhin, T. Ghosh, F.-C. Hsu, and J. Taneja (2021). Annual time series of global VIIRS nighttime lights derived from monthly averages: 2012 to 2019. *Remote Sensing* 13(5), 922.
- EOG (2022). Annual VIIRS night light version 2. data retrieved from the Earth Observaion Group, [https://eogdata.mines.edu/products/vnl/#annual\\_v2](https://eogdata.mines.edu/products/vnl/#annual_v2).
- ERMA (2009). Rwanda state of environment and outlook report 2009. Technical report, Rwanda Environment Management Authority.
- ERMA (2021). Rwanda state of environment and outlook report 2021. Technical report, Rwanda Environment Management Authority.
- FAO (2019). FAO framework on rural extreme poverty: Towards reaching Target 1.1 of the Sustainable Development Goals. Technical report, FAO.
- Fatima, F. and N. Yoshida (2018). Revisiting the poverty trend in rwanda: 2010/11 to 2013/14. *World Bank Policy Research Working Paper* (8585).
- GFCD (2015). Global Forest Change 2000–2021, The FAO portal to monitor Water Productivity through Open access of Remotely sensed derived data. data retrieved from the FAO Water Productivity Open-access portal, [https://wapor.apps.fao.org/home/WAPOR\\_2/1](https://wapor.apps.fao.org/home/WAPOR_2/1).
- GFCD (2022). Global Forest Change 2000–2021 Data Download. Annually upload de-forestation data and user notes are availble here, <https://storage.googleapis.com/earthenginepartners-hansen/GFC-2021-v1.9/download.html>.
- Ghanem, D., P. H. Sant’Anna, and K. Wüthrich (2022). Selection and parallel trends. *arXiv preprint arXiv:2203.09001*.
- Gibson, J., S. Olivia, G. Boe-Gibson, and C. Li (2021). Which night lights data should we use in economics, and where? *Journal of Development Economics* 149, 102602.
- Goodman-Bacon, A. (2021). Difference-in-differences with variation in treatment timing. *Journal of Econometrics* 225(2), 254–277.
- Gross-Camp, N. D., A. Martin, S. McGuire, and B. Kebede (2015). The privatization of the Nyungwe National Park Buffer Zone and implications for adjacent communities. *Society & Natural Resources* 28(3), 296–311.

- Hansen, M. C., P. V. Potapov, R. Moore, M. Hancher, S. A. Turubanova, A. Tyukavina, D. Thau, S. V. Stehman, S. J. Goetz, T. R. Loveland, et al. (2013). High-resolution global maps of 21st-century forest cover change. *science* 342(6160), 850–853.
- Heß, S., D. Jaimovich, and M. Schündeln (2021). Environmental effects of development programs: Experimental evidence from west african dryland forests. *Journal of Development Economics* 153, 102737.
- Hijmans, R. J. (2015). GLAD, Database of Global Administrative Areas, version 2.8. data retrieved from Stanford Earthworks, <https://earthworks.stanford.edu/catalog/stanford-vm033tb3847>.
- Jennings, G. (2016). Global outlook on walking and cycling report update. Technical report, UNEP.
- Kim, P. and E. Dumitrescu (2010). Share the road: Investment in walking and cycling road infrastructure. Technical report, UNEP.
- Lloyd, C. T., H. Chamberlain, D. Kerr, G. Yetman, L. Pistoiesi, F. R. Stevens, A. E. Gaughan, J. J. Nieves, G. Hornby, K. MacManus, et al. (2019). Global spatio-temporally harmonised datasets for producing high-resolution gridded population distribution datasets. *Big Earth Data* 3(2), 108–139.
- Macharia, D., L. MacDonald, L. Mugabo, K. Donovan, W. Brooks, S. Gudissa, A. Noriega, C. Barstow, K. Dickinson, and E. Thomas (2022). Mixed methods study design, pre-analysis plan, process evaluation and baseline results of trailbridges in rural Rwanda. *Science of the Total Environment* 838, 156546.
- Mukuralinda, A., M. Ndayambaje, A. Iiyama, B. Ndoli, D. Musana, D. Garrity, and S. Ling (2016). Taking to scale tree bases systems in Rwanda to enhance food security, restore degraded land, improve resilience to climate change and sequester carbon. Technical report, World Agroforestry Centre.
- Nawaz, S. and N. Iqbal (2020). The impact of unconditional cash transfer on fuel choices among ultra-poor in Pakistan: quasi-experimental evidence from the Benazir income support program. *Energy Policy* 142, 111535.
- NISR (2022). RPHC4 thematic report: Population size, structure and distribution. Technical report, National Institute of Statistics of Rwanda.
- Pérez-Sindín, X. S., T.-H. K. Chen, and A. V. Prishchepov. Remote sensing applications: Society and environment.
- Potapov, P. and M. Weissee (2022). Assessing trends in tree cover loss over 20 years of data. <https://www.globalforestwatch.org/blog/data-and-research/tree-cover-loss-satellite-data-trend-analysis/>.
- Rambachan, A. and J. Roth (2022). A more credible approach to parallel trends. Technical report, Working Paper.
- RoRMoE (2019). Rwanda Forest Cover Mapping. Technical report, Rwanda Environment Management Authority.
- Shirley, K., A. Noriega, D. Levin, and C. Barstow (2021). Identifying water crossings in rural Liberia and Rwanda using remote and field-based methods. *Sustainability* 13(2), 527.

- Stevens, F. R., A. E. Gaughan, C. Linard, and A. J. Tatem (2015). Disaggregating census data for population mapping using random forests with remotely-sensed and ancillary data. *PloS one* 10(2), e0107042.
- Sun, L. and S. Abraham (2021). Estimating dynamic treatment effects in event studies with heterogeneous treatment effects. *Journal of Econometrics* 225(2), 175–199.
- The World Bank (2020). Poverty. data retrieved from Poverty and Inequality Platform, [povertydata.worldbank.org](https://povertydata.worldbank.org).
- Thomas, E., A. Bradshaw, L. Mugabo, L. MacDonald, W. Brooks, K. Dickinson, and K. Donovan (2021). Engineering environmental resilience: A matched cohort study of the community benefits of trailbridges in rural Rwanda. *Science of The Total Environment* 771, 145275.
- UNDESA (2021). Reconsidering rural development. Technical report, United Nations Department of Economic and Social Affairs.
- Wilebore, B., M. Voors, E. H. Bulte, D. Coomes, and A. Kontoleon (2019). Unconditional transfers and tropical forest conservation: evidence from a randomized control trial in Sierra Leone. *American Journal of Agricultural Economics* 101(3), 894–918.
- WorldPop (2022). Population counts: Unconstrained individual countries 2000-2020 (100m resolution). data retrieved from the WorldPop Hub, <https://hub.worldpop.org/geodata/country?iso3=RWA>.

## A Forest Use in Rwanda

Rwanda saw a rapid decline in its forests over the 20th century. FAO defined forest land, an area of at least .5 hectares with 10% canopy cover, dropped from 25% of Rwanda's territory in 1960 to 9% in 2007 (ERMA, 2009). Forests were replaced by terraced farm holdings, leaving Rwanda the most densely populated non-island African country, with average household plot sizes of just 0.76 hectares (Fatima and Yoshida, 2018). Since 2009 to 2021, deforestation trends have turned around<sup>3</sup>. According to the government of Rwanda the total forest area increased by 5%, equivalent to 1.4% of Rwanda's land area (ERMA, 2021), however according to the FAO, who have a more stringent definition of forest, their was just a 3% increase in forest.<sup>4</sup> While there was in net forest gain, 15.7% of existing forest cover was lost and there is serious degradation of remaining forests and unprofessional management of new forest plantations. 24% of forest land is less than 40% canopied (ERMA, 2021). There is still remaining pristine montane tropical forest in national parks and reserves, but the growth in forest area has been driven by forest plantations of eucalyptus, pine and other fast growing dry rainforest species, mostly where montane tropical forests historically were. Plantations now account for 42% of all forest land in Rwanda, with 60% more plantation than remaining montane forest. 28% of plantations are in woodlots smaller than 2 hectares (RoRMoE, 2019). Besides plantations, farmers practice agroforestry, especially in the areas with denser population and smaller farm lots. Farmers intensively shift land between agricultural, livestock and wood production, and they scatter trees around homes and crop fields, as well as planting them along boundaries and terraces (Mukuralinda et al., 2016).

These plantations and other local trees supply Rwanda's principal energy source, biomass. 97.4% of Rwandans rely on forests for cooking in 2016, accounting for 80% of the energy mix in 2018 (ERMA, 2021). There are ambitious goals to transition to propane gas (reducing biomass use to 42%) and expand electricity access to the entire country, but estimated deficits in biofuel production are projected until 2050 without even more policy interventions (ERMA, 2021). Rwandans consumed twice as much wood as they produced in 2021. The results of the overuse and lack of forestry knowledge is that even though forest area is increasing, there is "extremely low forest productivity" (ERMA, 2021). The problem is most acute for small plantations managed by households, where forest stocks (measure of growth area potential) are almost 10 times as low compared to public or private institutional owners (ERMA, 2021). Over 28% of all canopy is in plots of 2 hectares or less (RoRMoE, 2019). 26% of biofuel comes from agroforestry sources and 43% from private sources (ERMA, 2021). While a handful of B2P trailbridges are adjacent to areas of tropical montane forest, the vast majority of nearby canopy is located in farm woodlots, contour hedgerows, boundary-planted trees, scattered trees in crop fields and home gardens (Mukuralinda et al., 2016).

Table B.5: Estimated Treatment Effects for Radiant Intensity in mW/SR, Different Specifications and Outcomes

	(1) NTL sum district time trends	(2) NTL sum by 10k pop, village time trends	(3) Square root NTL sum village time trends	(4) Log + 0.1 NTL sum, linear village time trends
Treatment-estimate	0.40** (0.20)	4.81** (1.90)	0.14** (0.06)	0.25** (0.12)
Pretrend-1	-0.05 (0.13)	0.57 (1.25)	-0.02 (0.03)	-0.05 (0.04)
Mean pre-treatment	3.01	36.94	1.51	0.57
Treated obs.	1175	1095	1095	1095
Total obs.	7370	7282	7282	7282
Treated villages	305	297	297	297
Total villages	670	662	662	662
Treated bridges	116	113	113	113
Total bridges	269	266	266	266
Year from	2012	2012	2012	2012
Year to	2022	2022	2022	2022

*Notes:* \*  $p < 0.1$ , \*\*  $p < 0.05$ , \*\*\*  $p < 0.01$ . Col. 1 includes as controls only completed or confirmed sites. Col. 2 adds to the main sample the unassessed villages identified in the needs assessment. Col. 3 adds to the main sample one large village next to the Nyungwe Forest National Park and the recently illuminated highway RN6. The standard errors are computed using the leave-out procedure recommended in Borusyak et al. (2021). Cohorts are constructed by combining treatment years from 2008 onwards so that each cohort has at least 15 bridges. All estimates account for year and village fixed effects, as well as unit-linear time trends.

Table B.6: Estimated Treatment Effects for Radiant Intensity in mW/SR, Different Samples

	(1) Complete or Confirmed	(2) Including unassessed	(3) Including large forest village
Treatment-estimate	0.58*** (0.20)	0.48*** (0.18)	0.95* (0.52)
Pretrend-1	-0.03 (0.11)	-0.10 (0.10)	-0.15 (0.12)
Mean pre-treatment	2.92	2.99	3.02
Treated obs.	1095	1095	1101
Total obs.	5082	7832	7293
Treated villages	297	297	298
Total villages	462	712	663
Treated bridges	113	113	113
Total bridges	182	289	266
Year from	2012	2012	2012
Year to	2022	2022	2022

*Notes:* \*  $p < 0.1$ , \*\*  $p < 0.05$ , \*\*\*  $p < 0.01$ . Col. 1–4 include controls sites either rejected after further assessment by B2P engineers, currently confirmed for construction, or in the RCT. Col. 1 estimate effects on village area sum of night time light radiant intensity in mW/SR. Col. 2–4 modify this by dividing by 10k population, taking the square root, or the natural logarithm plus 0.1, respectively. The standard errors are computed using the leave-out procedure recommended in Borusyak et al. (2021). Cohorts are constructed by combining treatment years from 2008 onwards so that each cohort has at least 15 bridges. All estimates account for year fixed effects and village fixed effects. Col. 2–4 additionally account for unit-linear time trends.

Table B.7: Estimated Treatment Effects for Population Outcomes

	(1)	(2)	(3)
	Population first difference, linear time trends	Log population linear time trends just confirmed	Log population linear time trends non-assessed
Treatment-estimate	10.536* (5.737)	0.033** (0.013)	0.033** (0.013)
Pretrend-1	2.072 (4.139)	-0.000 (0.004)	0.000 (0.004)
Mean pre-treatment	13.94	6.46	6.50
Treated obs.	673	673	673
Total obs.	9464	6650	10164
Treated villages	189	189	189
Total villages	676	475	726
Treated bridges	72	72	72
Total bridges	271	187	294
Year from	2007	2007	2007
Year to	2020	2020	2020

*Notes:* \*  $p < 0.1$ , \*\*  $p < 0.05$ , \*\*\*  $p < 0.01$ . Col. 1–2 include controls sites either rejected after further assessment by B2P engineers, currently confirmed for construction, or in the RCT. Col. 1–2 estimate effects on the log of village estimated total population. Standard errors are in parentheses. The standard errors are computed using the leave-out procedure recommended in Borusyak et al. (2021). Cohorts are constructed by combining treatment years from 2008 onwards so that each cohort has at least 15 bridges. All estimates account for year fixed effects and village fixed effects. Col. 2 additionally accounts for unit-linear time trends.

## B Robustness checks

### B.1 Additional Results on Night Time Light

### B.2 Additional Results on Population

### B.3 Additional Results on Deforestation

Specifications with fewer pre-treatment periods trade accuracy estimating village fixed effects for weaker assumptions, parallel trends do not extend as far back (However, see Figure X) for evidence of long-term parallel trends). In this instance, the GFCD has discontinuities in the time series, marginally in 2011 and by 300% in 2013 (Potapov and Weissee, 2022). Before the shift, detected deforestation events were predominately losses of heavily forested areas, where afterwards deforestation events of lightly forested areas (commonly associated with shifting agricultural practices) make up a larger part of the total. Table X shows the treatment effect is not an artifact of those shifts, and that the treatment effect persists at the other extreme of included pre-treatment periods.

Column 1 starts the time series in 2008 to include all bridges in the sample. The effect is approximately the same. Column 2 starts the panel in 2013, and the effect decreases. Some of this decrease can be attributed to dropping treated bridges between 2013-2014 that reported little deforestation after treatment. Column 3 restricts the time range to 2013-2017 and column

<sup>3</sup>Except in the East, where savannah woodland deforestation has accelerated, but is outside the focus of this study as trailbridge sites are not located in this area. Outside of national parks, only a fraction of 2009 levels of savanna woodland are left in 2019 (ERMA, 2021).

<sup>4</sup>The FAO and Rwanda have different definitions of forested areas, with Rwanda counting land of 25m<sup>2</sup> with 10% canopy cover, for 7250 km<sup>2</sup> in 2019. The FAO counted 2750 km<sup>2</sup> in 2019 (ERMA, 2021).

Table B.8: Estimated Treatment Effects for %-Canopy Deforested, Different Time Ranges

	(1)	(2)	(3)	(4)
	From 2008 year/#district FEs	From 2013 year/#district FEs	Treated 2013 to 2017 year/#district FEs	Treated 2018 to 2022 year/#district FEs
%-canopy	-0.17*** (0.06)	-0.13** (0.06)	-0.21*** (0.08)	-0.16* (0.09)
Pretrend-1	0.02 (0.07)	0.05 (0.08)	-0.05 (0.06)	0.08 (0.08)
Mean pre-treatment	0.32	0.42	1.08	0.43
Treated obs.	1209	1101	218	528
Total obs.	10140	6660	4718	3522
Treated villages	308	298	87	219
Total villages	676	666	674	587
Treated bridges	117	113	31	85
Total bridges	271	267	270	239
Year from	2008	2013	2011	2017
Year to	2022	2022	2017	2022

*Notes:* \*  $p < 0.1$ , \*\*  $p < 0.05$ , \*\*\*  $p < 0.01$ . Col. 1–4 include controls sites either rejected after further assessment by B2P engineers, currently confirmed for construction, or in the RCT. All columns estimate effects on yearly percent canopy cover deforested, calculated as the yearly village area deforested weighted by percent canopy cover of the deforested pixels in 2000 and divided by total village area forested in 2000. The standard errors are computed using the leave-out procedure recommended in Borusyak et al. (2021). Cohorts are constructed by combining treatment years from 2008 onwards so that each cohort has at least 15 bridges. Col. 1–4 account for year and bridge cluster fixed effects, and interacted year and district fixed effects.

4 similarly restricts to 2018-2022. Looking at either half or the main sample’s time range reveals similar estimates to having them all combined.

## C Mapped Outcome Data

Table B.9: Estimated Treatment Effects for Different Outcomes

	(1)	(2)	(3)
	Square meters deforestation event year#district FEs	Square root %-canopy deforested year#district FEs	Log+1 %-canopy deforested year#district FEs
%-canopy	-2336.63** (1016.32)	-4.53** (2.10)	-0.03** (0.01)
Pretrend-1	176.84 (889.98)	0.73 (2.45)	0.01 (0.01)
Mean pre-treatment	5313.47	19.63	1.09
Treated obs.	1181	1181	1181
Total obs.	8088	8088	8088
Treated villages	306	306	306
Total villages	674	674	674
Treated bridges	116	116	116
Total bridges	270	270	270
Year from	2011	2011	2011
Year to	2022	2022	2022

Notes: \* p<0.1, \*\* p<0.05, \*\*\* p<0.01. Col. 1–3 include controls sites either rejected after further assessment by B2P engineers, currently confirmed for construction, or in the RCT. Col. 1 estimate effects on the sum of the area of pixels reported deforested in square meters. Col. 2 uses the square root of the sum of the area of deforested pixels weighted by percent canopy cover in 2000. Col. 3 instead takes the natural logarithm plus one. The standard errors are computed using the leave-out procedure recommended in Borusyak et al. (2021). Cohorts are constructed by combining treatment years from 2008 onwards so that each cohort has at least 15 bridges. Col. 1–3 account for year and bridge cluster fixed effects, and interacted year and district fixed effects.

Table B.10: Estimated Treatment Effects for Percent Canopy Deforested, Different Specifications and Samples

	(1)	(2)	(3)	(4)	(5)
	Completed or Confirmed year#district FEs	Incl, unassessed year#district FEs	Main Sample non-rounded year year#district FEs	Main sample year FEs	Main sample district linear year trends
%-canopy	-0.16** (0.06)	-0.16** (0.06)	-0.17*** (0.06)	-0.16** (0.06)	-0.16*** (0.05)
Pretrend-1	-0.02 (0.06)	-0.01 (0.06)	0.04 (0.06)	0.03 (0.07)	0.05 (0.07)
Mean pre-treatment	0.35	0.37	0.40	0.37	0.37
Treated obs.	1139	1181	1318	1205	1181
Total obs.	7038	8688	8088	8112	8088
Treated villages	301	306	355	308	306
Total villages	590	724	674	676	674
Treated bridges	114	116	138	117	116
Total bridges	234	293	270	271	270
Year from	2011	2011	2011	2011	2011
Year to	2022	2022	2022	2022	2022

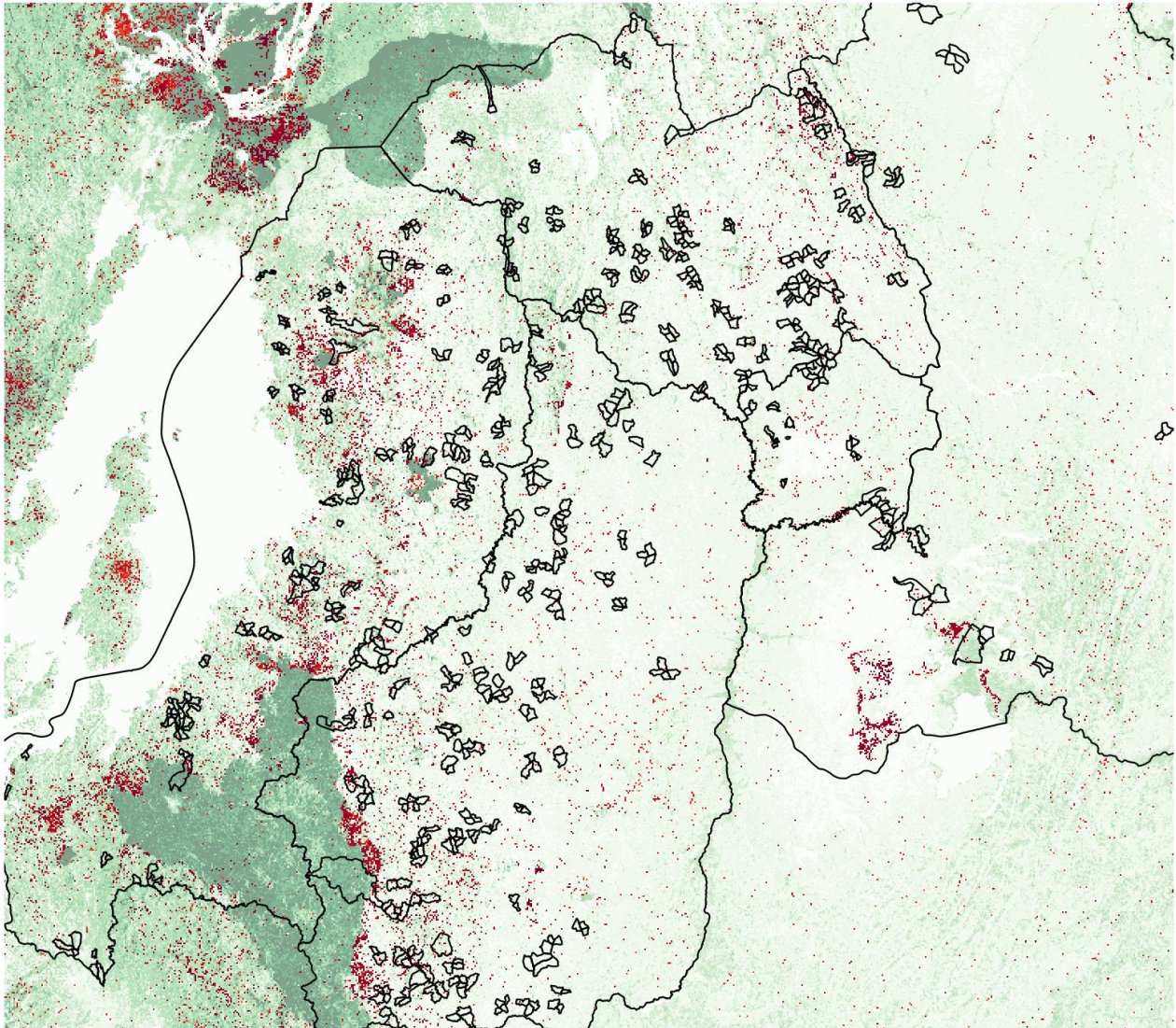
Notes: \* p<0.1, \*\* p<0.05, \*\*\* p<0.01. Col. 3–5 include controls sites either rejected after further assessment by B2P engineers, currently confirmed for construction, or in the RCT. Col. 1 only uses completed or confirmed as controls. Col. 2 adds to the main sample not yet assessed sites. All columns estimate effects on yearly percent canopy cover deforested, calculated as the yearly village area deforested weighted by percent canopy cover of the deforested pixels in 2000 and divided by total village area forested in 2000. Standard errors are in parentheses. The standard errors are computed using the leave-out procedure recommended in Borusyak et al. (2021). Cohorts are constructed by combining treatment years from 2008 onwards so that each cohort has at least 15 bridges. Col. 1–3,5 account for year and bridge cluster fixed effects, and interacted year and district fixed effects. Col. 4 controls for year and bridge cluster fixed effects, and district linear time trends.

Table B.11: Estimated Treatment Effects for Percent Canopy Deforested, Decomposing the Effect

	(1) Binary deforestation event year#district FEs	(2) Some deforestation %-canopy deforested year#bundled-district FEs	(3) Some deforestation log deforestation sqr meters year#bundled-district FEs
Treatment-estimate	-0.03 (0.03)	-0.25* (0.15)	-0.29** (0.13)
Pretrend-1	0.03 (0.03)	0.11 (0.17)	0.05 (0.15)
Mean pre-treatment	0.40	0.89	7.11
Treated obs.	1181	472	472
Total obs.	8088	3228	3228
Treated villages	306	199	199
Total villages	674	603	603
Treated bridges	116	95	95
Total bridges	270	260	260
Year from	2011	2011	2011
Year to	2022	2022	2022

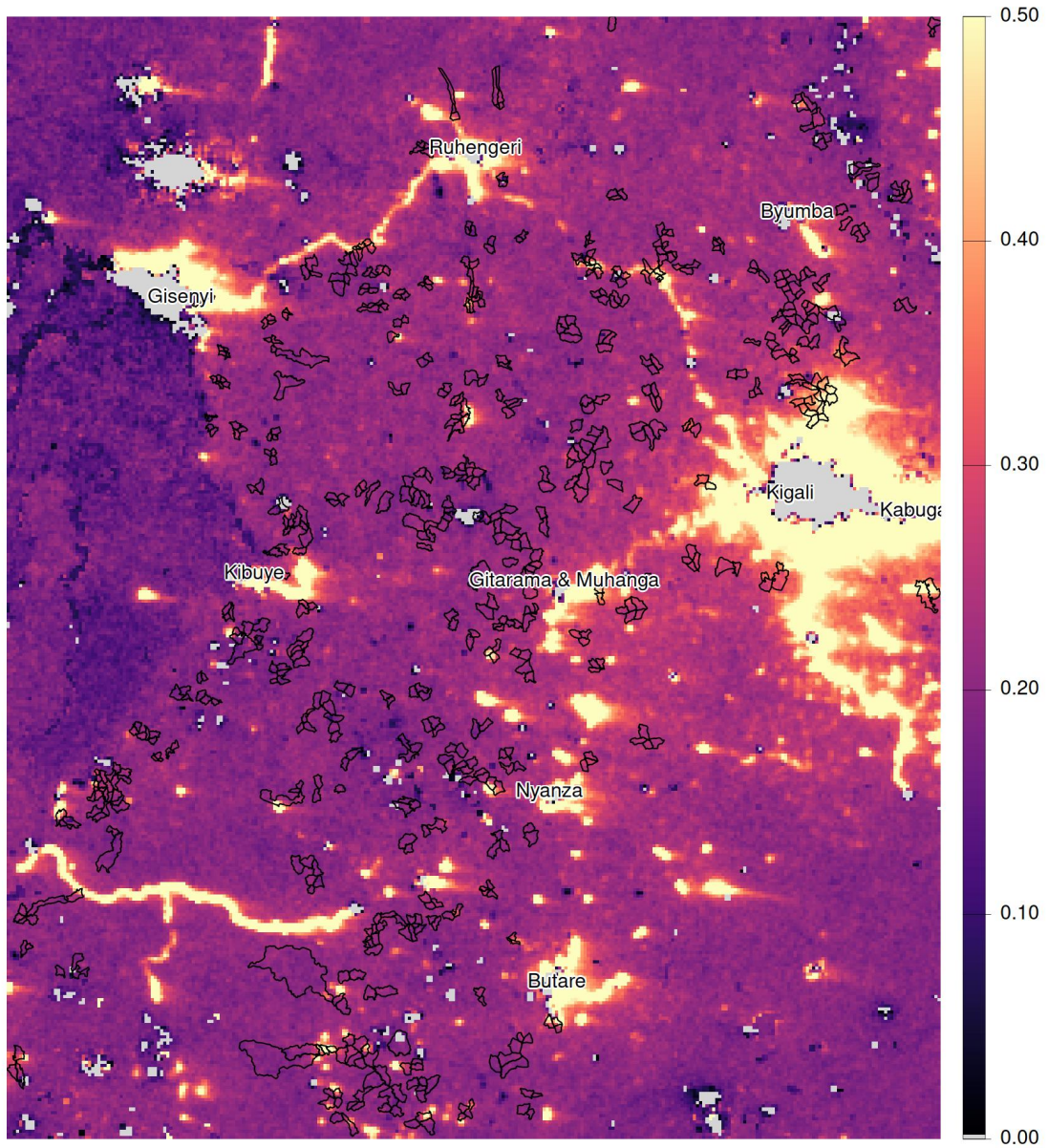
*Notes:* \*  $p < 0.1$ , \*\*  $p < 0.05$ , \*\*\*  $p < 0.01$ . Col. 1–3 include controls sites either rejected after further assessment by B2P engineers, currently confirmed for construction, or in the RCT. Col. 1–2 restrict the sample to only observations with some deforestation. Col. 1 estimates effects on whether any deforestation occurred. Col. 2 uses yearly percent canopy cover deforested, calculated as the yearly village area deforested weighted by percent canopy cover of the deforested pixels in 2000 and divided by total village area forested in 2000. Col. 3 uses the natural logarithm of the sum of the area of deforested pixels weighted by canopy cover in 2000. Standard errors are in parentheses. The standard errors are computed using the leave-out procedure recommended in Borusyak et al. (2021). Cohorts are constructed by combining treatment years from 2008 onwards so that each cohort has at least 15 bridges. Col. 1–3 account for year fixed effects, bridge cluster fixed effects. Col. 1 also accounts for interacted year and district fixed effects, while Col. 2–3 account for year and bundled-districts fixed effects.

Figure C.1: Deforestation and Percent Canopy Cover in 2000



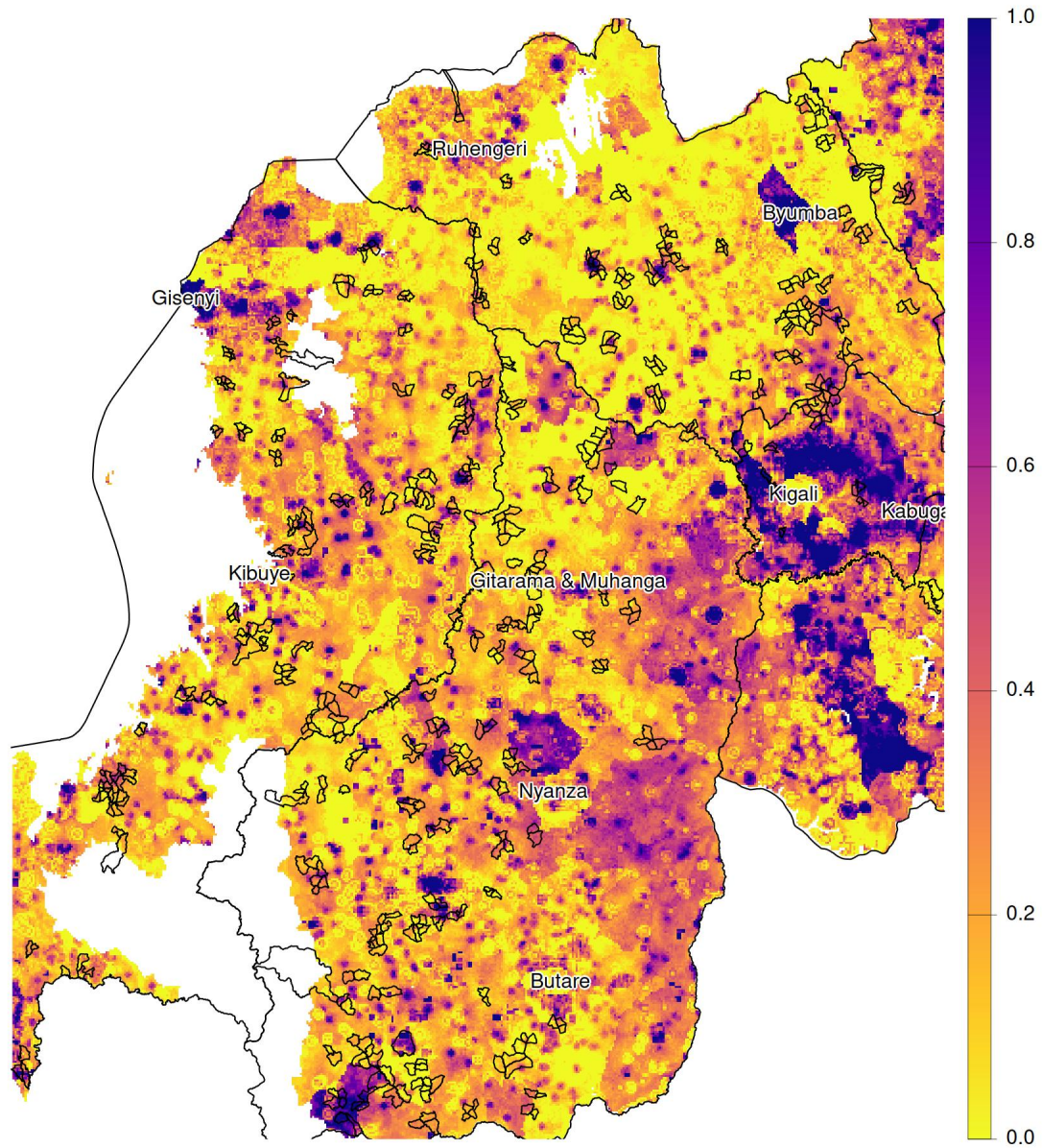
Darker colored warm pixels show more recent deforestation from 2000 to 2021. Sample villages are imposed over map. Rwandan political boundaries provided by GLAD.

Figure C.2: Difference between 2012-2014 Average Radiance and 2019-2021 Average Radiance



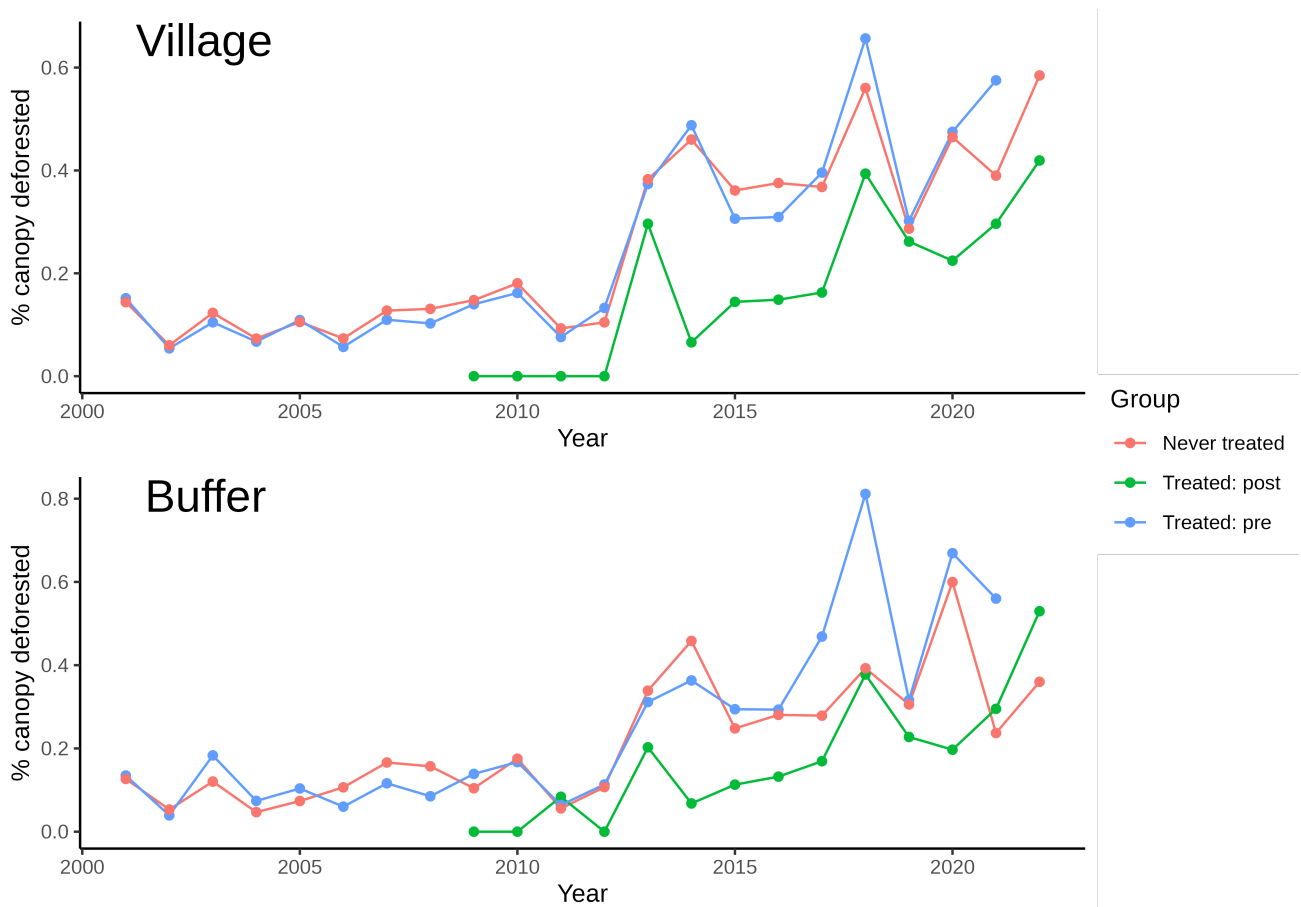
Scale is in  $nW/cm^2/sr$ . The values are top coded at .5 and bottom coded to 0, which is depicted as gray. Sample villages are imposed over map. The names of the twelve largest cities in Rwanda that fall in the depicted area are displayed. Rwandan political boundaries provided by GLAD.

Figure C.3: Fraction Change in Population Density by Hectare from 2012 to 2021



Scale is fraction change in population between 2012 and 2021. The values are top coded at 1 and bottom coded to 0. Sample villages are imposed over map. The names of the twelve largest cities in Rwanda that fall in the depicted area are displayed. Rwandan political boundaries provided by GLAD.

Figure C.4: Yearly Percentage Canopy Deforested by Treatment Status



Never treated are the preferred set of controls. Percentage canopy deforested is derived from the GFCD, and is the ratio of detected pixels of deforestation weighted by canopy in 2000 to the area of canopy in 2000. Rwandan political boundaries used in calculations were provided by GLAD.